

Supplementary Information

Exploring the Origin of White Emission in TAPC:Electron Transport Layer based Exciplex Devices

Insung Ha^{1,a)}, Hyun Woo Cho^{2,a)}, Hyung Joo Lee^{3,a)}, Ezhakudiyar Ravindran⁴⁾, P. Justin Jesuraj^{1,5)}, Jae Woo Lee⁶⁾, Chang Min Lee^{1,b)}, Chul Hoon Kim^{3,b)} and Seung Yoon Ryu^{1,7,b)}

¹Department of Physics, Dongguk University, Seoul 04620, Republic of Korea

²Department of Applied Physics, Korea University, Sejong 30019, Republic of Korea

³Department of Advanced Materials Chemistry, Korea University, Sejong 30019, Republic of Korea

⁴Department of Chemistry, SRM Institute of Science and Technology, Kattankulathur, India - 603 203

⁵Department of Physics and Nanotechnology, S.R.M. Institute of Science and Technology, Kattankulathur, India - 603 203

⁶Department of Electronics and Information Engineering, Korea University, Sejong City 30019, Republic of Korea

⁷Photoenergy Harvesting and Conversion Technology (*phct*), Dongguk University, Seoul 04620, Republic of Korea

^{a)}I. Ha, H.W. Cho and H.J. Lee contributed equally to this work.

^{b)}Authors to whom correspondence should be addressed: cm0404@dgu.ac.kr , chulhoon@korea.ac.kr, justie74@dongguk.edu

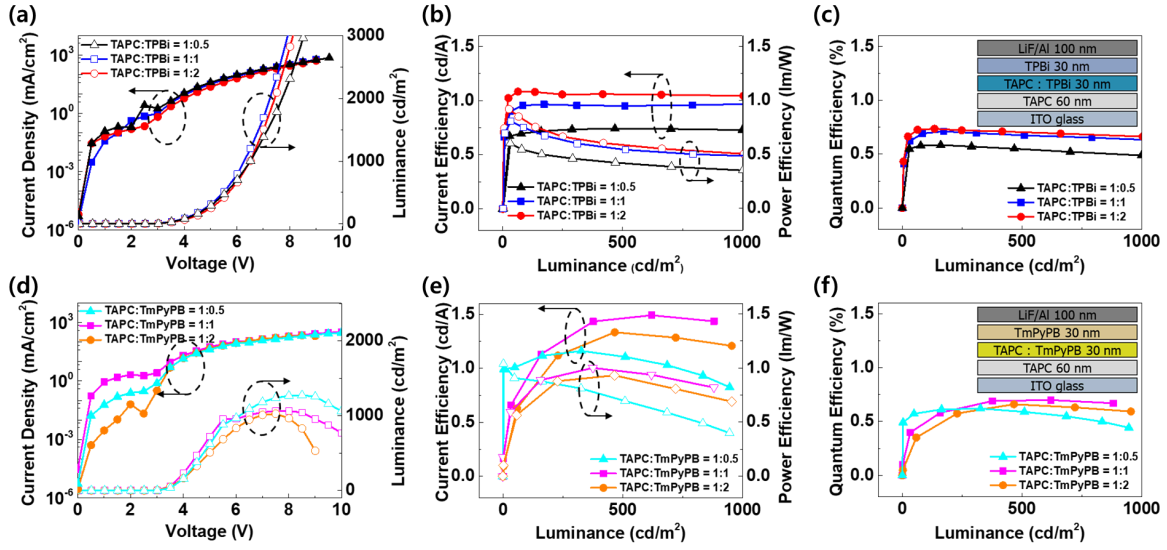


Fig. S1: Device performance of blue Ph-OLED for different ratios of electron transport material (ETM) thicknesses. a,d, Current density-voltage-luminance plots, b,e, current/power efficiency, and c,f, quantum efficiency of TPBi- and TmPyPB-based exciplex devices.

We varied the co-deposited layer ratio (HTL:ETL), with values of 1:0.5, 1:1, and 1:2, to obtain stable white emission. Adjusting the ratio of the co-deposited layer primarily influences exciplex formation relative to the ETL material ratio, thereby affecting the overall color coordinates and device performance. The current density (J) and luminescence (L) performance of all the devices at different voltages is shown in **Fig. S1**. All the devices showed the same turn-on voltage of 3 V. This low turn-on voltage indicates that the co-evaporation approach is better for achieving exciplex emission. Previous studies have reported much higher turn-on voltages, reaching 17 V or 20 V, since they employed a thicker EML layer.[1] Among the TAPC:TPBi devices, the device with a co-deposited layer ratio of 1:2 showed the best current efficiency and quantum efficiency, as shown in **Fig. S1b and S1c**. The efficiency roll-off observed in TmPyPB-based devices is likely due to the deeper HOMO level of TmPyPB, approximately 0.5 eV lower than that of TPBi, which restricts hole injection from TAPC into the ETL. This mismatch results in a more pronounced efficiency roll-off.[2] Research has demonstrated that incorporating a hole injection layer (HIL) or a gradually doped layer effectively reduces the injection barrier and mitigates efficiency roll-off. By improving charge balance and minimizing non-radiative losses, such approaches significantly suppress efficiency roll-off.[3] Additionally, using dipolar-doped HTL has been shown to effectively suppress charge accumulation and enable high-efficiency OLEDs.[4]

However, our focus was on comparing different ETLs, and thus, we did not pursue tuning the injection barrier in this study.

Additionally, the current density-voltage characteristics reveal a noticeable inflection around 7V in TmPyPB-based devices, further suggesting injection limitations under higher voltage conditions. The superior performance appears to originate from the better charge balance between electrons and holes for radiative emission. Similarly, the 1:1 TAPC:TmPyPB co-deposited layer showed better performance because of better charge balance between TAPC and TmPyPB.[1a, 5]

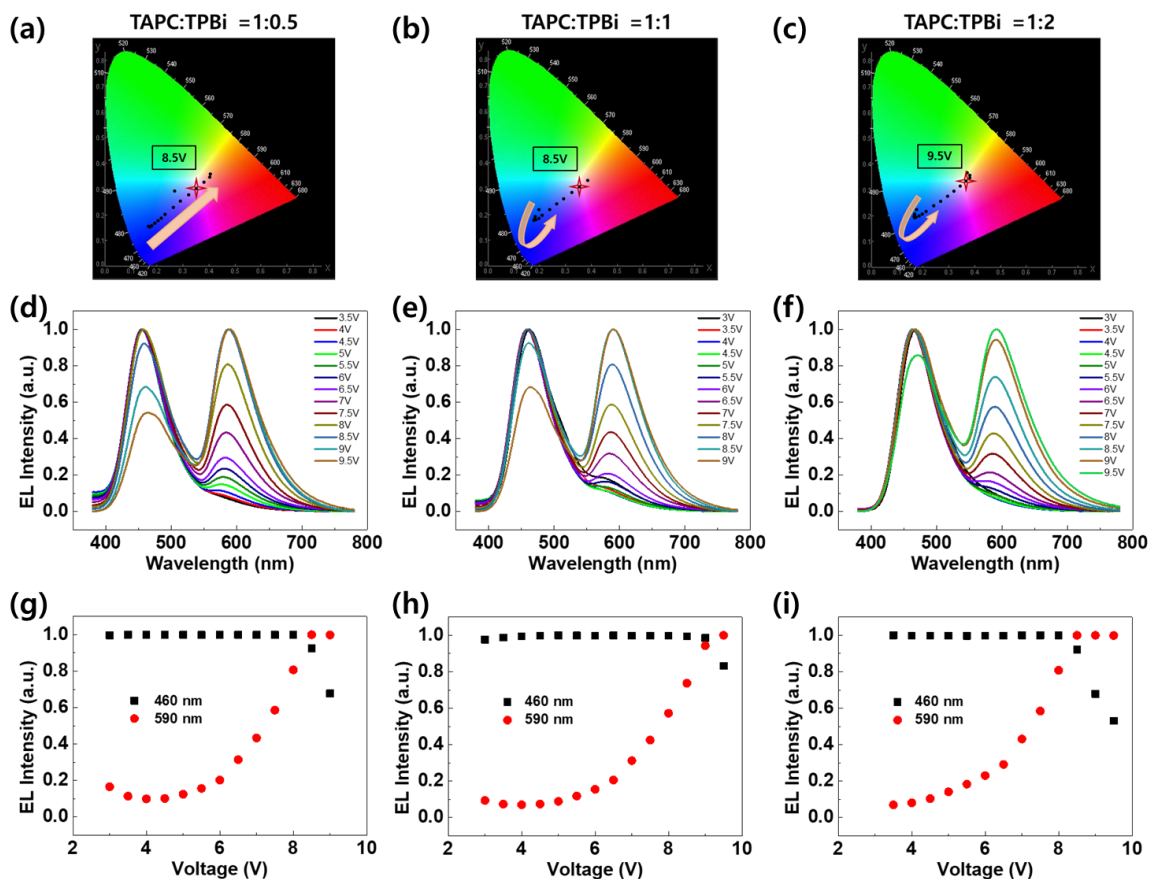


Fig. S2: Electroluminescence (EL) intensity profiles for different TAPC-TPBi ratios of TPBi-based exciplex devices without an EBL. a-c, CIE 1931 color analysis by varying the applied voltage and d-f, corresponding EL intensities for different proportions of TPBi and for different applied voltages.

The color coordinates and EL emission spectra of TAPC devices are shown in **Fig. S2**. At voltages below 6 V, for all ratios, the primary emission was observed at 460 nm, corresponding to blue emission dominated by excitons generated within the TAPC. As the voltage increased beyond 6 V, an additional emission peak appeared at approximately 600 nm, attributed to exciplex or electromer formation at the interface between TAPC and TPBi. This voltage-dependent change in the emission spectra contributed to the transition from blue to white emission.

For the 1:1 TAPC:TPBi ratio, the color coordinates approached the white emission region at 8.5 V. At this voltage, the 460 nm blue emission band was observed to have a lower intensity than the 600 nm band, indicating a balance between the two emission components that is essential for achieving white emission. In the device with a TAPC:TPBi ratio of 1:2,

the dominance of the 600 nm emission band over the 460 nm band was observed at a slightly higher voltage (9.5 V). This delayed transition can be attributed to the higher proportion of TPBi, which enhances blue emission originating from the TAPC HTL.[1a] As a result, a higher voltage is required to achieve the balance between blue and red emissions necessary for white light. Conversely, in the device with a TAPC:TPBi ratio of 1:0.5, the transition to dominance of the 600 nm emission over the 460 nm band occurred at a lower voltage (8.5 V). The reduced TPBi content in this device lowers the blue emission contribution, facilitating an earlier transition to white emission as the voltage increases.

These observations suggest that the ratio of TAPC to TPBi strongly influences the voltage threshold at which white emission is achieved by altering the relative contributions of blue and red emissions. This behavior is further corroborated by the evolution of the CIE coordinates, which shift from blue-dominated regions at low voltages to near-white regions as the voltage increases.

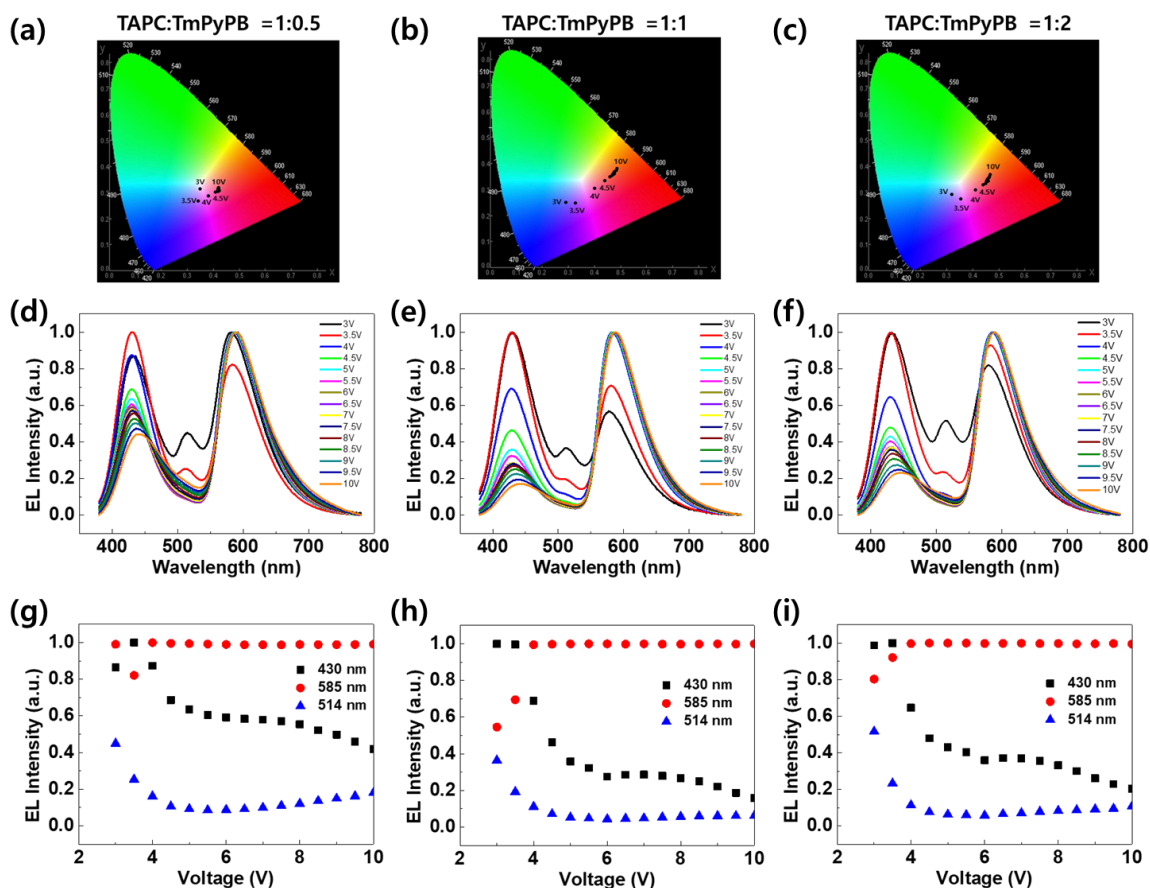


Fig. S3: Electroluminescence (EL) intensity profiles for different TAPC-TmPyPB ratios of TmPyPB-based exciplex devices without an EBL. a-c, CIE 1931 color analysis by varying the applied voltage and d-f, corresponding EL intensities for different proportions of TmPyPB under different applied voltages.

For comparison, the color coordinates and EL spectra of the TAPC:TmPyPB devices are shown in **Fig. S3**. Unlike the TAPC:TPBi devices, the TAPC:TmPyPB devices exhibited a primary emission peak at 430 nm at low voltages (below 4 V). As the voltage increased, this emission shifted towards a higher wavelength of 570 nm, with a gradual red shift observed across all devices. This red shift can be attributed to the transition from the low-lying charge transfer state of TAPC to the ground-state potential surface of TmPyPB, as previously reported.[6] For TAPC:TmPyPB devices with a 1:1 ratio, the color coordinates closest to white emission were observed at 4 V, corresponding to the point where the primary emission shifted to approximately 580 nm. At higher voltages, the intensity of the emission at 430 nm decreased, while the peak at 570 nm became dominant, signaling exciplex formation. In contrast, for devices with a 1:2 ratio, the color coordinates were closer to white emission at a lower voltage of 3 V, likely due to the improved charge mobility of TmPyPB. Similarly, the

device with a 1:0.5 ratio exhibited white emission at 3 V, which can be attributed to better exciplex formation under these conditions.

Overall, while TAPC:TPBi devices exhibited abrupt changes in color coordinates with increasing voltage, TAPC:TmPyPB devices demonstrated comparatively stable emission characteristics. This stability arises from the better charge mobility of TmPyPB, which facilitates more consistent exciplex formation.[5] Thus, devices employing TmPyPB as the ETL material hold a distinct advantage over TPBi-based devices in achieving stable white emission.

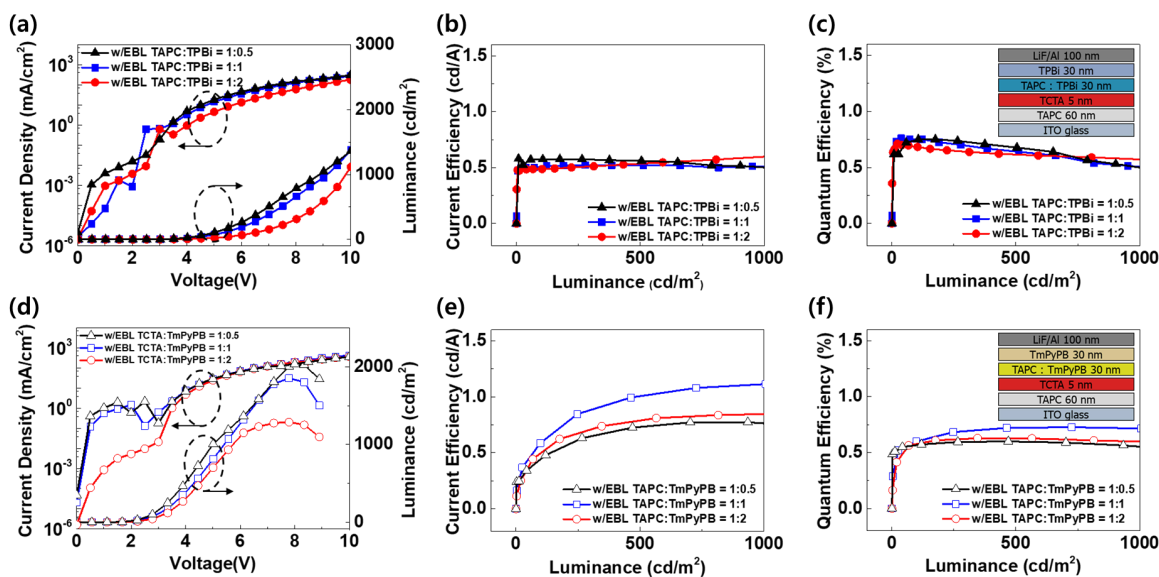


Fig. S4: Device performance of blue Ph-OLED under different ratios of electron transport material (ETM) thicknesses with a electron blocking layer (EBL). a,d, Current density-voltage-luminance plots, b,e, current efficiency, and c,f, quantum efficiency of TPBi- and TmPyPB-based exciplex devices.

The devices with an electron-blocking layer (EBL) exhibited a slightly delayed current injection compared with those without an EBL, as shown in **Fig. S4**. Consequently, the lower efficiency observed in devices with an EBL can be attributed to charge imbalance caused by the insertion of the additional functional layer, rather than poor current injection.

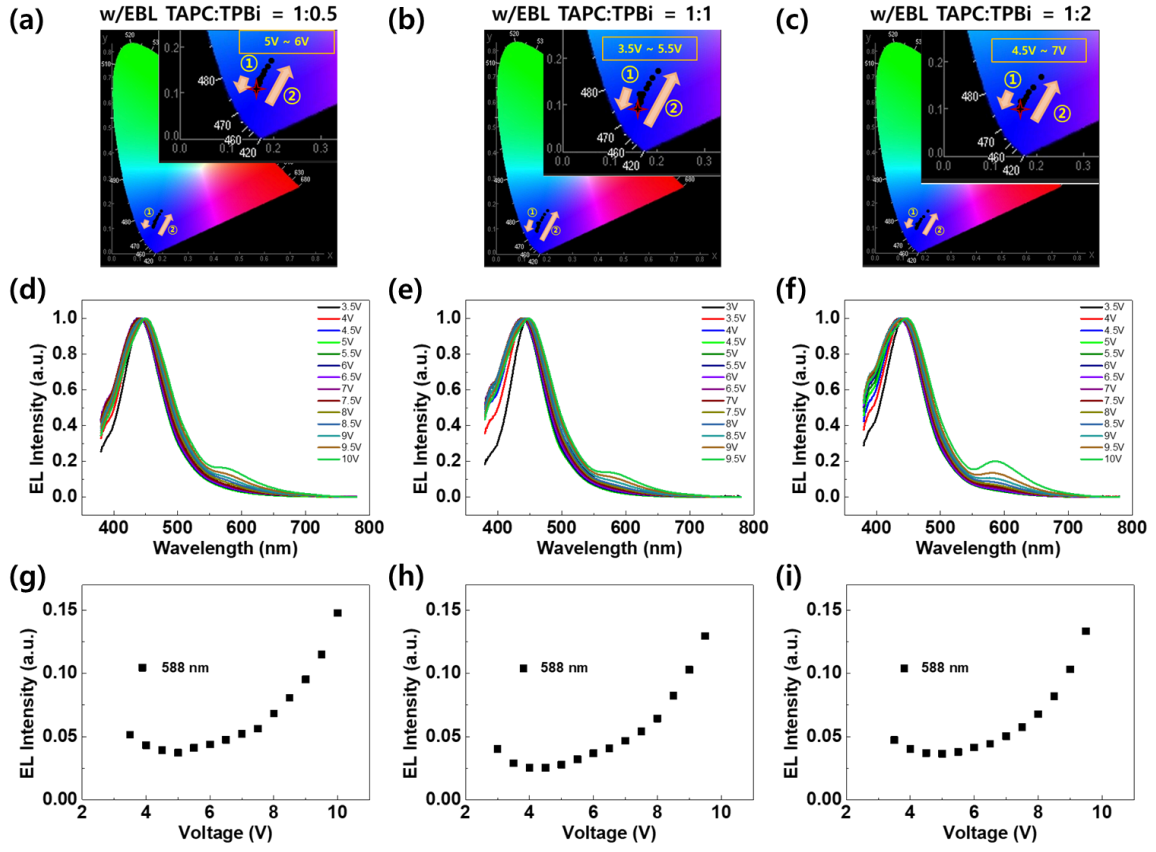


Fig. S5: Electroluminescence (EL) intensity profiles for different TAPC-TPBi ratios of TPBi-based exciplex devices with an EBL. a-c, CIE 1931 color analysis by varying the applied voltage and d-f, corresponding EL intensities for different proportions of TPBi under different applied voltages.

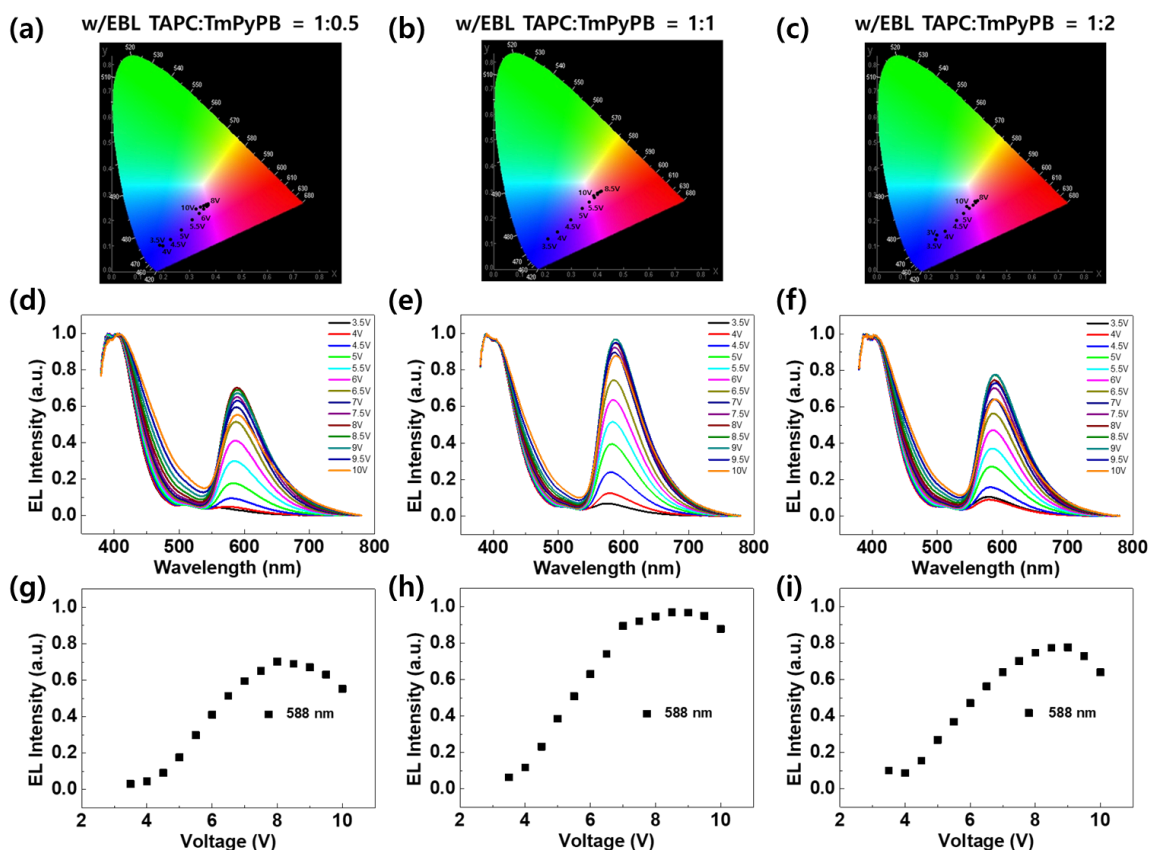


Fig. S6: Electroluminescence (EL) intensity profiles for different TAPC-TmPyPB ratios of TmPyPB-based exciplex devices with an EBL. a-c, CIE 1931 color analysis by varying the applied voltage and d-f, corresponding EL intensities for different proportions of TmPyPB under different applied voltages.

Unlike the results observed without an EBL, the EL intensity for each voltage remained relatively stable in the presence of an EBL, as depicted in **Fig. S5** and **S6**. In both TPBi- and TmPyPB-based devices, the presence of an EBL decelerated hole injection, leading to a reduction in electromer generation and a diminished change in the EL intensity for driving at various voltages. Notably, the blue component arose from the formation of an exciplex at the TAPC/ETL (TPBi and TmPyPB) heterointerface, while the yellow and red components of the EL spectrum at 590 nm were attributed to the formation of electromers within the bulk of TAPC, respectively. This conclusion is supported by the absence of the 590 nm emission in the PL spectra, its exclusive observation during EL operation, and its voltage-dependent intensity increase. These characteristics are consistent with the behavior of electromers, which form under electrical excitation and are influenced by the charge injection dynamics and device architecture.[1a] To investigate this in more detail, we conducted further optical

analyses, including TRPL measurements.

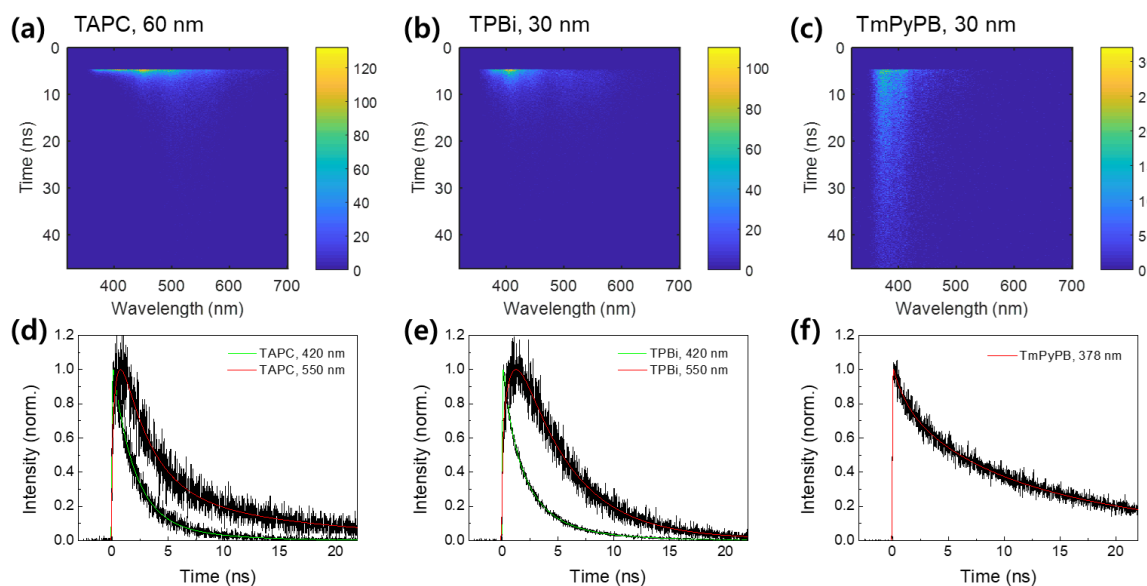


Fig. S7: Time-resolved photoluminescence (TRPL) spectra of TAPC, TPBi, and TmPyPB in films and their TRPL profiles at representative detection wavelengths.

Table S1. Multi-exponential fitting results of TRPL profiles of single-layered films recorded at representative detection wavelengths.

Sample	λ (nm)	A_1 (%) ¹⁾	τ_1 (ps)	A_2 (%)	τ_2 (ns)	A_3 (%)	τ_3 (ns)	τ_{avg} (ns) ²⁾
TAPC	420	84.3	1820	15.7	5.62			2.42
	550	-38.0	404	47.9	2.71	14.2	15.1	3.29
TPBi	425	27.1	807	60.9	2.28	12.0	6.32	2.36
	550	-37.6	794	61.8	4.69	0.59	42.9	2.85
TmPyPB	378	16.8	1020	27.7	5.02	55.6	18.8	12.0

1) Negative amplitude indicates an increase.

2) Only decay components were used to determine corresponding averaged lifetimes.

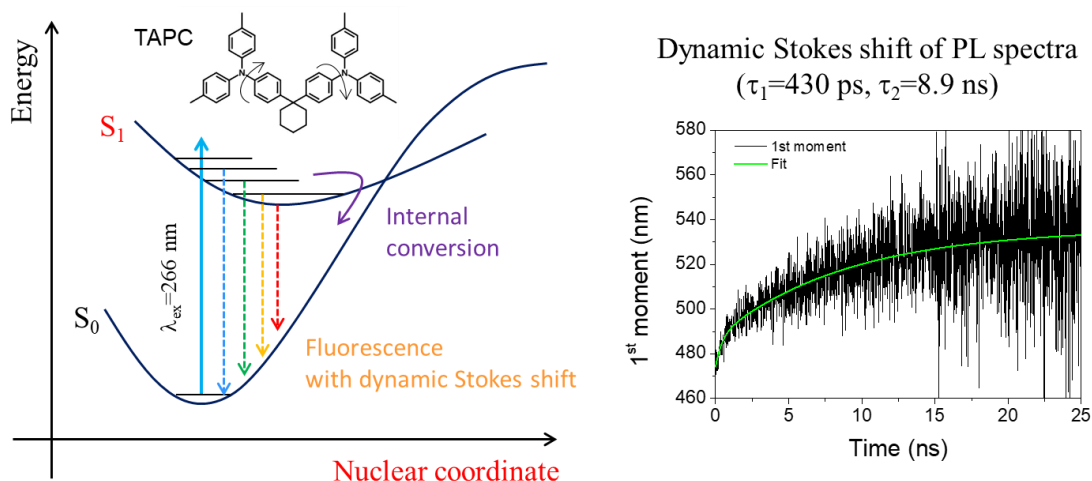


Fig. S8: Schematic of the structural relaxation dynamics of TAPC in an excited state and the multi-exponential fitting result of the intensity-weighted center wavelength (1st moment). Twisting motions of triphenyl rings can induce slow dynamic Stokes shift and subsequent internal conversion.

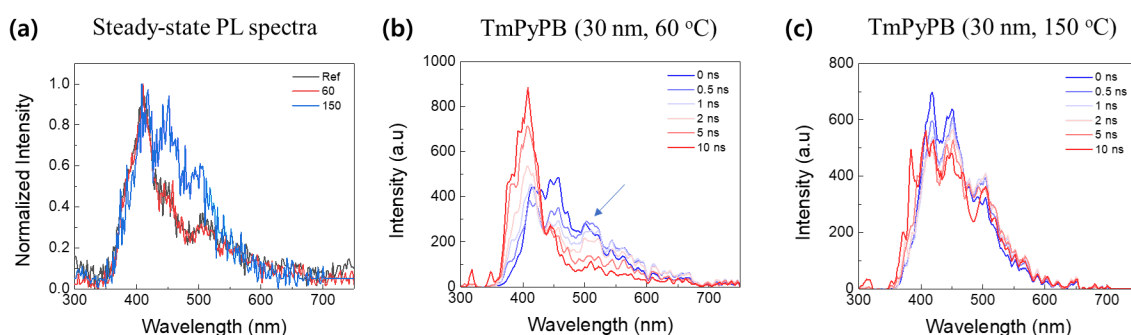
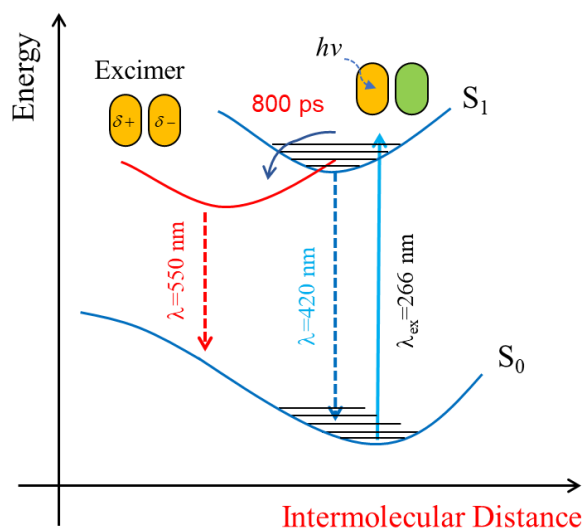


Fig. S9: Steady-state and time-resolved photoluminescence spectra of TmPyPB in film. The spectral band at around 450 nm becomes dominant as the annealing temperature increases (60 °C and 150 °C).



TRPL profiles at monomer and excimer bands

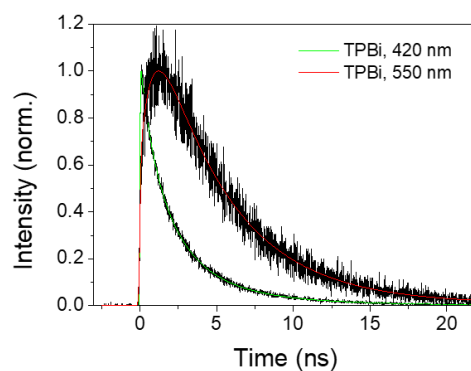


Fig. S10: Schematic of the structural relaxation dynamics of TPBi in an excited state and steady-state, and time-resolved photoluminescence spectra of TmPyPB in film. The spectral band at around 480 nm is dependent on the annealing temperature (60 °C and 150 °C).

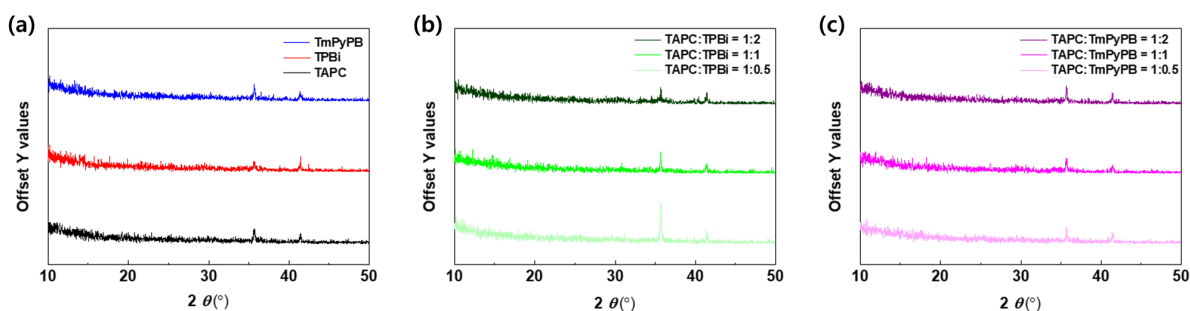


Fig. S11: X-ray diffraction (XRD) patterns of single films (TAPC, TPBi and TmPyPB) and the co-deposited films (TAPC:TPBi and TAPC:TmPyPB with ratio of 1:0.5, 1:1 and 1:2)

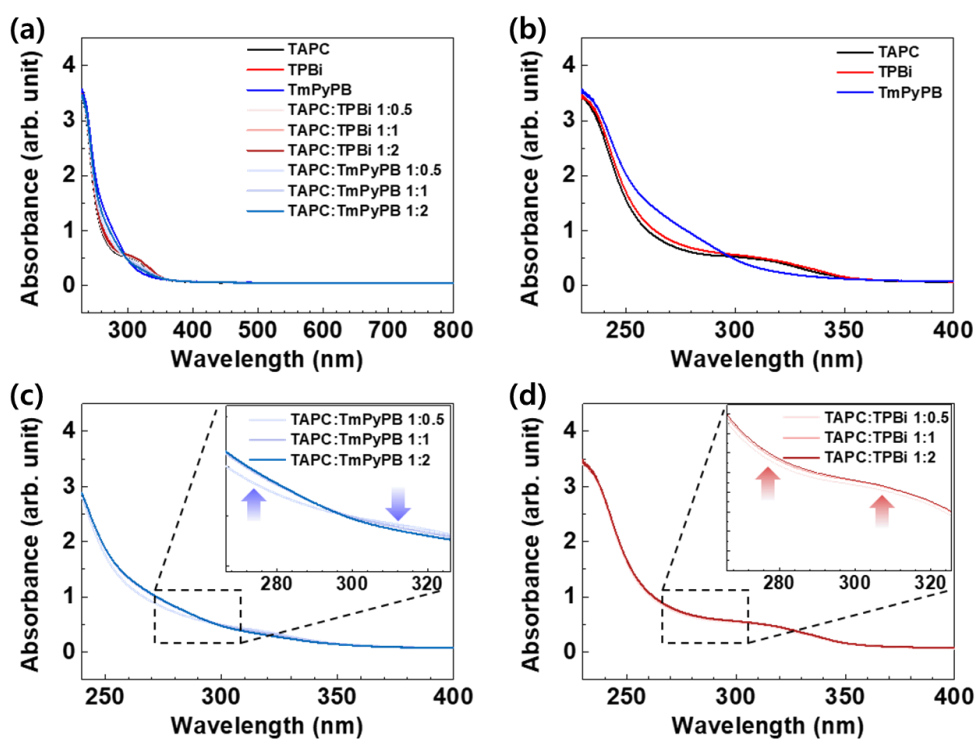


Fig. S12: UV-vis absorption spectra of single films (TAPC, TPBi and TmPyPB) and the co-deposited films (TAPC:TPBi and TAPC:TmPyPB with ratio of 1:0.5, 1:1 and 1:2)

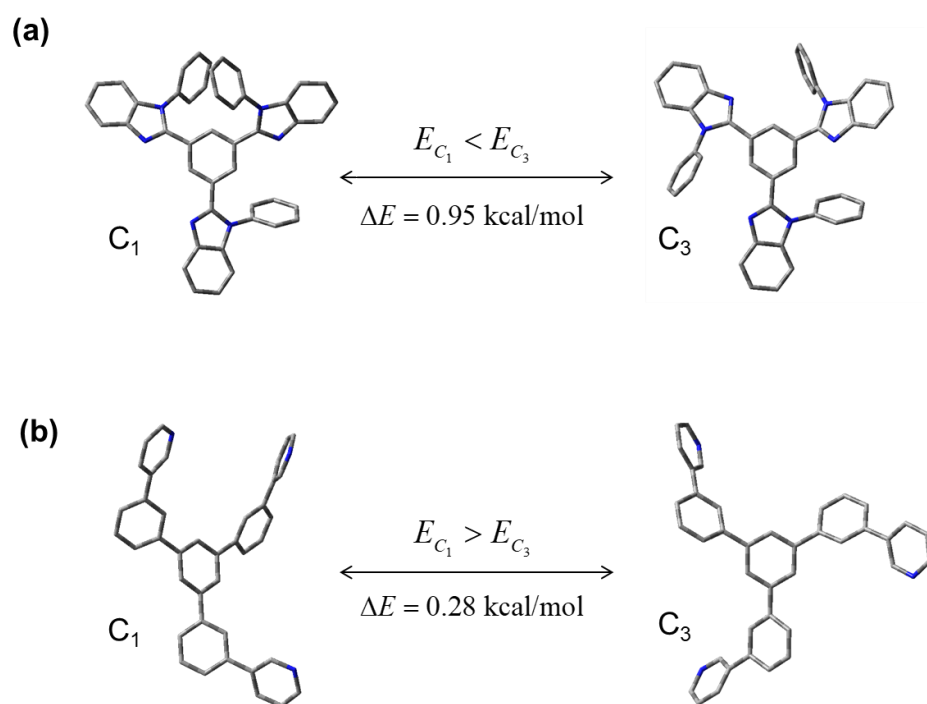


Fig. S13: The C_1 and C_3 conformers of (a) TPBi [7] and (b) TmPyPB. For clarity, all hydrogen atoms have been omitted.

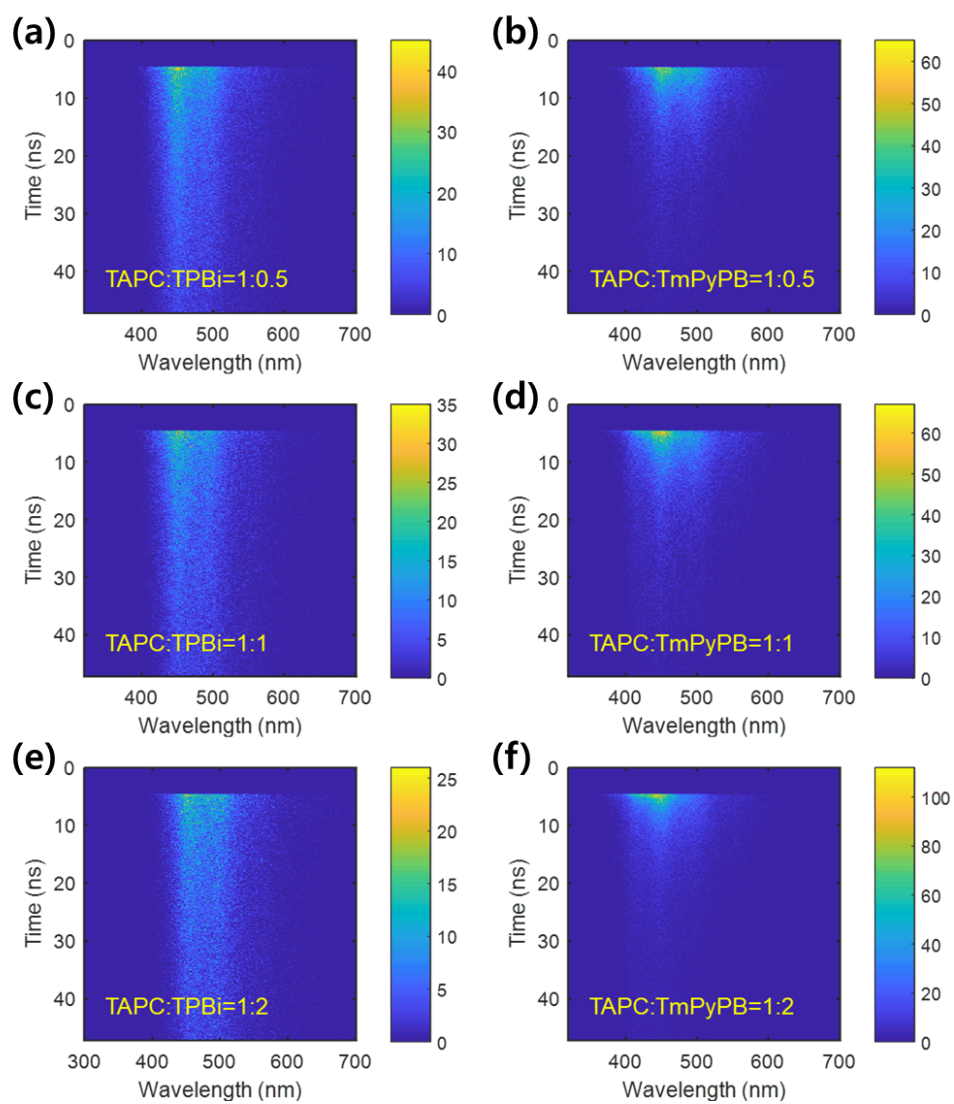


Fig. S14: Time-resolved photoluminescence spectra of TAPC:TPBi and TAPC:TmPyPB films with different mixing ratios.

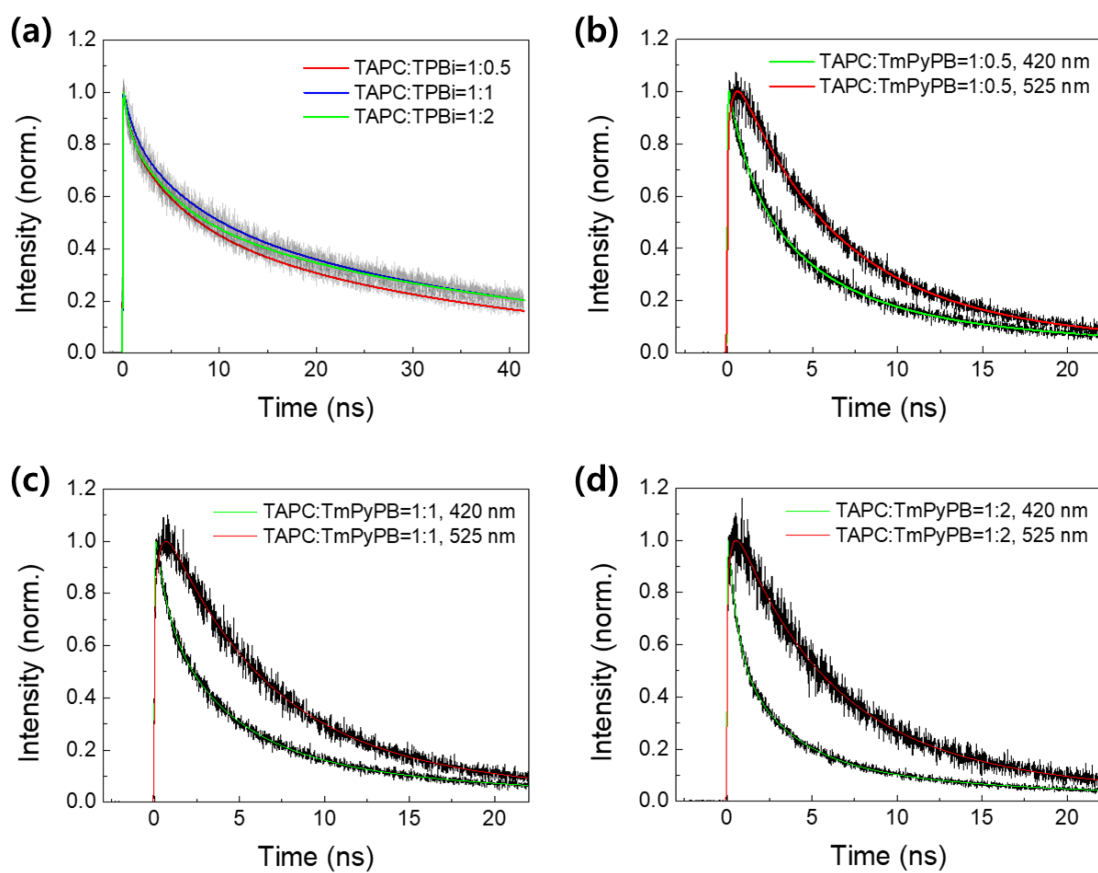


Fig. S15: Time-resolved photoluminescence profiles of TAPC:TPBi and TAPC:TmPyPB films with different mixing ratios.

Table S2. Multi-exponential fitting results of TRPL profiles of the co-deposited films recorded at representative detection wavelengths.

Sample	Ratio	λ (nm)	A_1 (%) ¹⁾	τ_1 (ps)	A_2 (%)	τ_2 (ns)	A_3 (%)	τ_3 (ns)	τ_{avg} (ns) ²⁾
TAPC:TPBi	1:0.5	454	16.9	766	32.1	5.74	51.0	35.3	20.0
	1:1	456	15.1	1160	29.1	6.49	55.9	40.3	24.6
	1:2	458	15.6	553	31.3	5.05	53.1	41.7	23.8
TAPC:TmPyPB	1:0.5	420	26.8	1144	53.5	4.38	19.6	18.9	6.35
		525	-22.5	319	61.6	5.47	16.0	18.7	6.28
	1:1	420	29.0	762	51.9	3.95	19.0	18.8	5.85
		525	-24.4	350	62.4	5.84	13.3	20.8	6.32
	1:2	420	44.7	562	41.9	3.19	13.5	17.6	3.96
		525	-22.0	280	61.2	5.25	16.8	17.0	6.00

1) Negative amplitude indicates an increase.

2) Only decay components were used to determine corresponding averaged lifetimes.

In contrast to TAPC:TPBi films, which exhibit relatively stable behavior, the TAPC:TmPyPB films show a pronounced variation in the average PL lifetime at 420 nm with increasing TmPyPB ratio. This variation is closely related to the contribution of exciplex character in the PL spectrum. In particular, the bathochromic shift in the PL spectrum at time-zero is most pronounced for the 1:0.5 ratio, as shown in **Fig. 4**. The average PL lifetime of 6.2 ns at 420 nm for the 1:0.5 ratio is comparable to the lifetime observed at 525 nm, suggesting that TAPC:TmPyPB (1:0.5) forms a relatively well-stacked exciplex structure. This well-organized structure results in the longer average PL lifetime, which can be interpreted as the lifetime of the H-type exciplex.[8] In contrast, for the 1:2 ratio, the average PL lifetime at 420 nm is similar to that of the TAPC single-layer film (Table S1), indicating weaker excitonic interaction between the two molecules. In this case, the PL transition of the TAPC moiety dominates in the mixed film, leading to a shorter average lifetime of approximately 3 ns at 420 nm. These observations highlight the influence of molecular interactions and structural organization within the co-deposited films on the photophysical properties of TAPC:ETL systems.

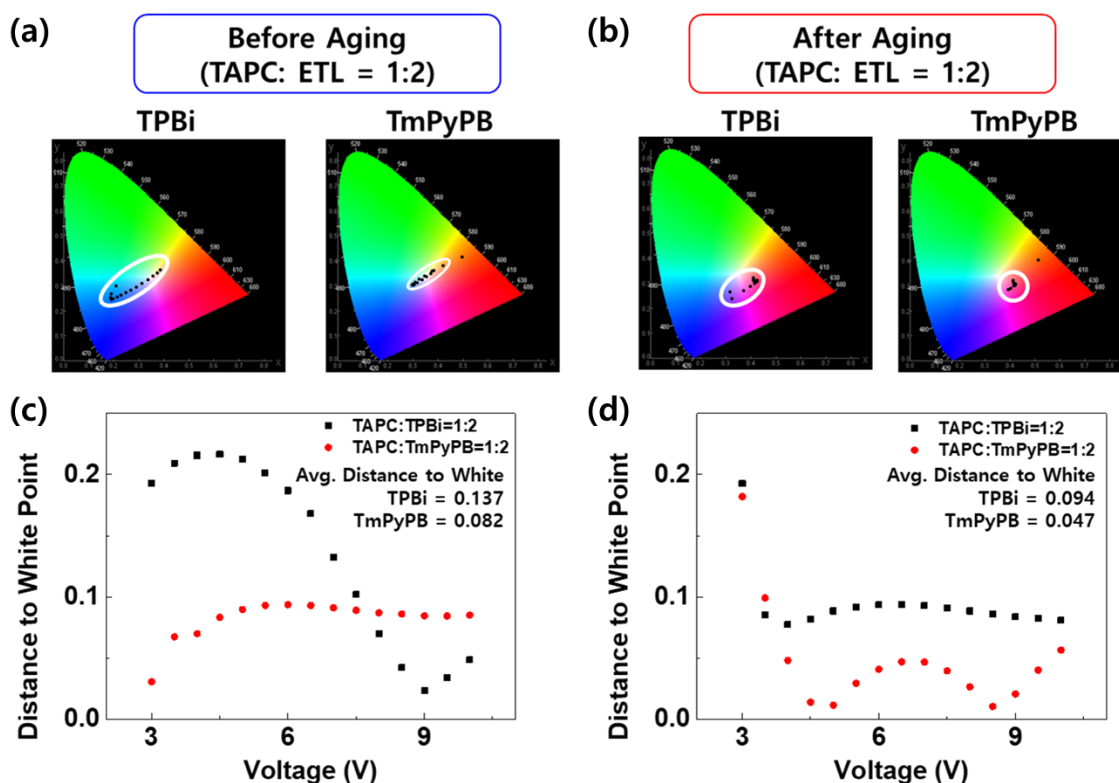


Fig. S16: CIE 1931 color coordinate and the distance to white (in CIE 1931) of TPBi- and TmPyPB-based exciplex devices before and after aging. a,b, CIE 1931 color coordinate before and after aging and **c,d,** distance to white point in CIE 1931 color coordinate for different applied voltages.

To examine the stability of exciplex formation and white emission, we aged the devices by one time operation as shown in **Fig. S13**. Distances between the color coordinates at each voltage and the white coordinates are shown. White coordinate A, situated at (1/3, 1/3) on the CIE coordinate, was compared with color coordinate B obtained at each voltage. The resultant coordinates C, derived by subtracting B from A, were represented as (X, Y). To quantify the white coordinate distance between A and B, the formula $\sqrt{X^2 + Y^2}$ was used. Interestingly, for both TPBi- and TmPyPB-based devices, the color coordinates were much closer to white emission after aging. The aged TmPyPB-based device showed higher stability at higher voltages because of the higher carrier mobility in TmPyPB compared with TPBi. **Figure S13d** shows a comparison of color coordinates between TPBi- and TmPyPB-based devices that were aged.

This improvement was attributed to the initial current flow filling some of the defects and voids in the device, leading to changes in the exciplex and recombination zone.

Consequently, upon subsequent operations, electrons and holes followed more stable pathways with fewer defects, modulating exciplex formation and stabilizing the color coordinates. However, over extended usage, the accumulation of defect-driven degradation caused noticeable shifts in the emission spectra and color coordinates, as shown in **Fig. S13**. While this highlights the device's lower long-term stability compared to fully optimized OLED structures, it also suggests a unique application for such devices in optical sensing. Specifically, the observed emission color shifts could serve as functional indicators for environmental monitoring or failure detection. For instance, color changes could correspond to specific environmental factors, such as heat, oxygen, or humidity exposure, transforming this limitation into a valuable feature for non-display applications. This novel approach leverages the device's instability to provide real-time sensing capabilities, potentially opening new avenues for exciplex-based device designs beyond conventional display technologies.

References

- [1] a) S. Yang, M. Jiang, *Chemical Physics Letters* **2009**, *484* (1-3), 54; b) J. Kalinowski, G. Giro, M. Cocchi, V. Fattori, P. Di Marco, *Applied Physics Letters* **2000**, *76* (17), 2352.
- [2] a) C. Murawski, K. Leo, M. C. Gather, *Advanced Materials* **2013**, *25* (47), 6801; b) J. Li, B. Qiao, S. Zhao, D. Song, C. Zhang, Z. Xu, *Organic Electronics* **2020**, *83*, 105756; c) W. H. Lee, D. H. Kim, P. J. Jesuraj, H. Hafeez, J. C. Lee, D. K. Choi, T.-S. Bae, S. M. Yu, M. Song, C. S. Kim, *Materials Research Express* **2018**, *5* (7), 076201.
- [3] a) H. Z. Siboni, H. Aziz, *Organic Electronics* **2013**, *14* (10), 2510; b) W.-L. Huang, M.-C. Tsai, T.-H. Wang, S.-Y. Chu, P.-C. Kao, *Organic Electronics* **2022**, *111*, 106666.
- [4] Y. Noguchi, A. Hofmann, W. Brütting, *Advanced Optical Materials* **2022**, *10* (21), 2201278.
- [5] a) K.-H. Chou, T.-H. Chen, X.-Q. Huang, C.-S. Huang, C.-H. Chang, C.-T. Chen, J.-H. Jou, *Materials Advances* **2023**, *4* (5), 1335; b) G. W. Kim, Y. H. Son, H. I. Yang, J. H. Park, I. J. Ko, R. Lampande, J. Sakong, M.-J. Maeng, J.-A. Hong, J. Y. Lee, *Chemistry of Materials* **2017**, *29* (19), 8299.
- [6] W. Yip, D. H. Levy, *The Journal of Physical Chemistry* **1996**, *100* (28), 11539.
- [7] J. Calimano, F. Li, J. Florián, D. M. Piñero-Cruz, T. R. Fielitz, R. J. Holmes, J. W. Ciszek, *The Journal of Physical Chemistry C* **2020**, *124* (43), 23716.
- [8] A. Garci, Y. Beldjoudi, M. S. Kodaimati, J. E. Hornick, M. T. Nguyen, M. M. Cetin, C. L. Stern, I. Roy, E. A. Weiss, J. F. Stoddart, *Journal of the American Chemical Society* **2020**, *142* (17), 7956.